

# Efficient Deep Learning for Massive MIMO Channel State Estimation



Mason del Rosario  
Doctoral Qualifying Examination

May 2021

## Background

Role of CSI in MIMO

## CSI Estimation

Convolutional Neural Networks

## Prior Work #1: SphNet

Spherical Normalization

## Prior Work #2: MarkovNet

Differential Encoding

## Proposed Work: CsiNet-SoftQuant

Soft-to-Hard Vector Quantization

# Background

---

Feedback-based estimation of channel state information in MIMO networks.

Massive MIMO uses numerous antennas to endow transceivers with spatial diversity.

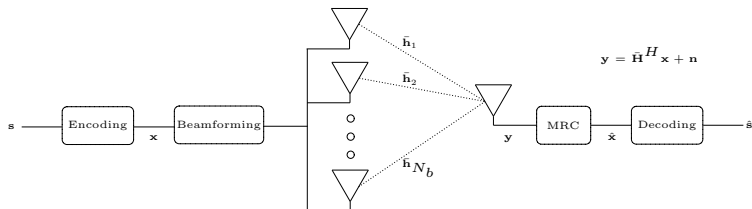
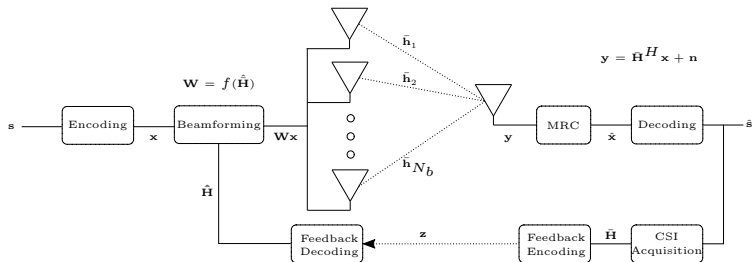


Figure: Example multi-antenna transmitter (BS, gNB) and single-antenna user equipment (UE) and relevant system values.

In OFDM, the fading coefficients between the Tx/Rx antennas constitute **Channel State Information (CSI)**,  $\bar{\mathbf{H}}$ . For  $n_T$  transmit antennas and  $n_f$  subcarriers,

$$\bar{\mathbf{H}} = \begin{bmatrix} h_{1,1} & h_{1,2} & \dots & h_{1,n_T} \\ h_{2,1} & h_{2,2} & \dots & h_{2,n_T} \\ \vdots & \vdots & \vdots & \vdots \\ h_{n_f,1} & h_{n_f,2} & \dots & h_{n_f,n_T} \end{bmatrix} \in \mathbb{C}^{n_f \times n_T}$$

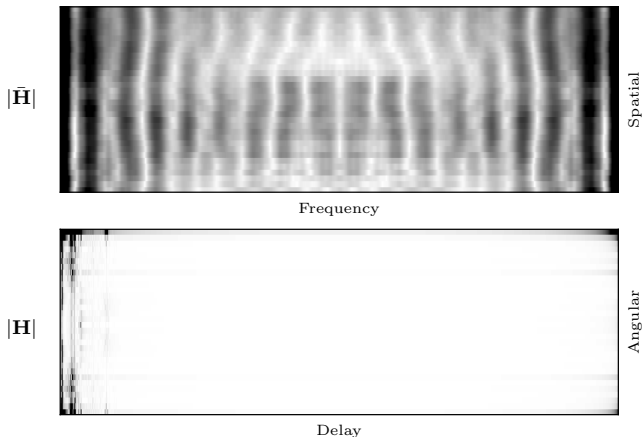
However, transmitting  $\bar{\mathbf{H}}$  is costly. Instead, generate **CSI Estimates**,  $\hat{\bar{\mathbf{H}}}$ , based on **compressed feedback**,  $\mathbf{z}$ .



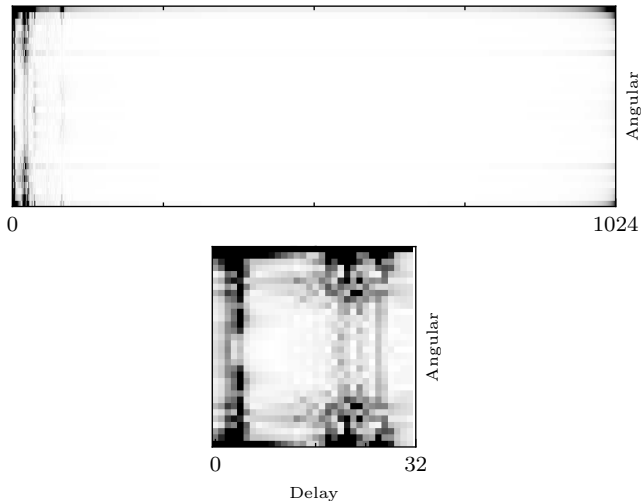
Denote the 2D inverse FFT of  $\bar{\mathbf{H}}$  as

$$\mathbf{H} = \mathbf{F}^H \bar{\mathbf{H}} \mathbf{F}.$$

While  $\bar{\mathbf{H}}$  is used for beamforming,  $\mathbf{H}$  is more amenable to compression.



Given the sparsity of  $\mathbf{H}$  (angular-delay domain), we choose to encode a truncated  $\mathbf{H}$ .





1. Compressed Sensing
2. Convolutional Neural Networks

Find a low-dimensional representation of sparse data,  $\mathbf{h}$ , by a linear transform,  $\mathbf{A}$ ,

$$\mathbf{y} = \mathbf{A}\mathbf{h} + \mathbf{n},$$

where  $\mathbf{h}$  is a vectorized CSI measurement,  $\mathbf{A}$  is the measurement matrix, and  $\mathbf{n}$  is an additive noise vector.

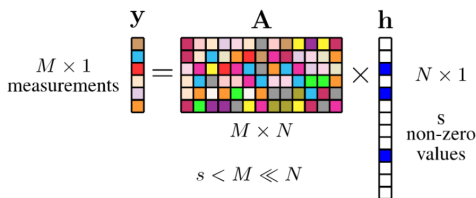


**Figure:** Compressed sensing via random measurement matrix  $\mathbf{A}$  (from [1]).

CS theory relies on the following assumptions:

1. The sparsity of the signal to be estimated must meet a certain level.
2. The **Restricted Isometry Criterion (RIC)** must be met. For  $\delta \in [0, 1]$ ,

$$(1 - \delta)\|\mathbf{h}\|_2^2 \leq \|\mathbf{A}\mathbf{h}\|_2^2 \leq (1 + \delta)\|\mathbf{h}\|_2^2$$

Generally, CS approaches address two major issues:

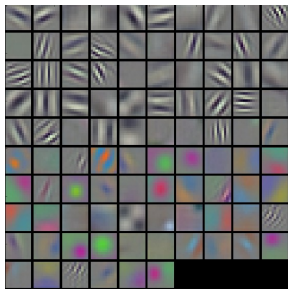
1. The design of the measurement matrix,  $\mathbf{A}$  (stochastic or deterministic).
2. The recovery of  $\hat{\mathbf{h}}$  given  $\mathbf{A}$  and  $\mathbf{y}$  (e.g., Matching Pursuit, Orthogonal Matching Pursuit [2]).

Generally, CS approaches address two major issues:

1. The design of the measurement matrix,  $\mathbf{A}$  (stochastic or deterministic).
2. The recovery of  $\hat{\mathbf{h}}$  given  $\mathbf{A}$  and  $\mathbf{y}$  (e.g., Matching Pursuit, Orthogonal Matching Pursuit [2]).

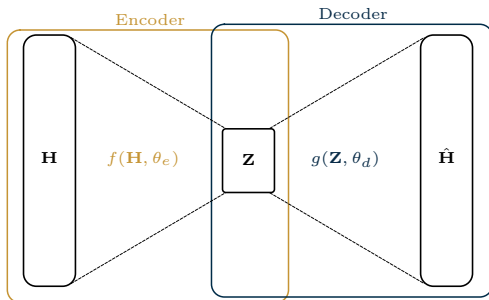
**Problem: Recovery algorithms are iterative; complexity scales with  $M$ .**

- ▶ CNNs = state-of-the art performance in image processing
- ▶ Multiple layers of trainable linear functions followed nonlinear ‘activation’ functions.
- ▶ No assumptions on sparsity, RIC. Instantaneous decoding.



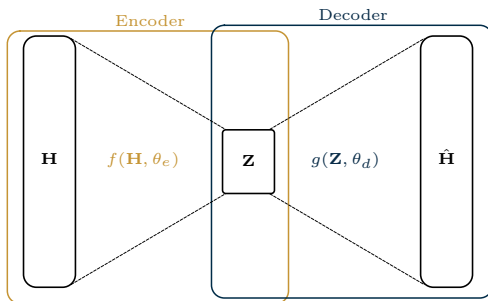
An autoencoder learns a latent code  $\mathbf{Z}$  with **compression ratio**,

$$\text{CR} = \frac{\dim(\mathbf{Z})}{\dim(\mathbf{H})} \text{ s.t. } \dim(\mathbf{Z}) < \dim(\mathbf{H}).$$



An autoencoder learns a latent code  $\mathbf{Z}$  with **compression ratio**,

$$\text{CR} = \frac{\dim(\mathbf{Z})}{\dim(\mathbf{H})} \text{ s.t. } \dim(\mathbf{Z}) < \dim(\mathbf{H}).$$

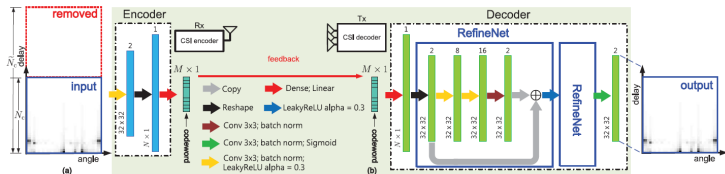


The encoder/decoder parameters  $\theta_e, \theta_d$  are updated via a stochastic optimizer to minimize the **mean-squared error**,

$$\operatorname{argmin}_{\theta_e, \theta_d} \frac{1}{N} \sum_{i=1}^N \|\mathbf{H}_i - g(f(\mathbf{H}_i, \theta_e), \theta_d)\|^2.$$



- CNN-based autoencoder for learned CSI compression and feedback [3]



Metrics used are:

► **Normalized Mean-squared Error**

$$\text{NMSE} = \frac{1}{N} \sum_i^N \frac{\|\mathbf{H}_i - \hat{\mathbf{H}}_i\|_2^2}{\|\mathbf{H}_i\|_2^2}$$

► **Cosine Similarity**

$$\rho = \frac{1}{N} \sum_i^N \frac{|\bar{\mathbf{H}}_i \cdot \hat{\hat{\mathbf{H}}}_i|}{\|\bar{\mathbf{H}}_i\|_2 \|\hat{\hat{\mathbf{H}}}_i\|_2}$$

Metrics used are:

► **Normalized Mean-squared Error**

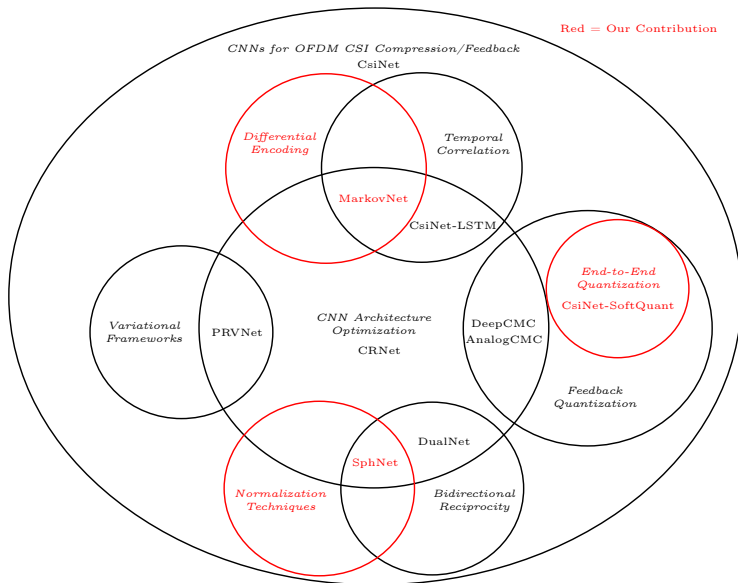
$$\text{NMSE} = \frac{1}{N} \sum_i \frac{\|\mathbf{H}_i - \hat{\mathbf{H}}_i\|_2^2}{\|\mathbf{H}_i\|_2^2}$$

► **Cosine Similarity**

$$\rho = \frac{1}{N} \sum_i \frac{|\bar{\mathbf{H}}_i \cdot \hat{\mathbf{H}}_i|}{\|\bar{\mathbf{H}}_i\|_2 \|\hat{\mathbf{H}}_i\|_2}$$

CNN-based approaches outperform CS-based approaches at comparable compression ratios.

$\gamma$	Methods	Indoor		Outdoor	
		NMSE	$\rho$	NMSE	$\rho$
1/4	LASSO	-7.59	0.91	-5.08	0.82
	BM3D-AMP	-4.33	0.80	-1.33	0.52
	TVAL3	-14.87	0.97	-6.90	0.88
	CS-CsiNet	-11.82	0.96	-6.69	0.87
	CsiNet	<b>-17.36</b>	<b>0.99</b>	<b>-8.75</b>	<b>0.91</b>
1/16	LASSO	-2.72	0.70	-1.01	0.46
	BM3D-AMP	0.26	0.16	0.55	0.11
	TVAL3	-2.61	0.66	-0.43	0.45
	CS-CsiNet	-6.09	0.87	-2.51	0.66
	CsiNet	<b>-8.65</b>	<b>0.93</b>	<b>-4.51</b>	<b>0.79</b>
1/32	LASSO	-1.03	0.48	-0.24	0.27
	BM3D-AMP	24.72	0.04	22.66	0.04
	TVAL3	-0.27	0.33	0.46	0.28
	CS-CsiNet	-4.67	0.83	-0.52	0.37
	CsiNet	<b>-6.24</b>	<b>0.89</b>	<b>-2.81</b>	<b>0.67</b>
1/64	LASSO	-0.14	0.22	-0.06	0.12
	BM3D-AMP	0.22	0.04	25.45	0.03
	TVAL3	0.63	0.11	0.76	0.19
	CS-CsiNet	-2.46	0.68	-0.22	0.28
	CsiNet	<b>-5.84</b>	<b>0.87</b>	<b>-1.93</b>	<b>0.59</b>



## Prior Work #1: SphNet

---

Power-based normalization for improved CSI reconstruction accuracy.

Most works perform **minmax scaling** – Take the extrema ( $\mathbf{H}_{\min}, \mathbf{H}_{\max}$ ) of the real and imaginary channels,

$$\mathbf{H}_{n,\text{minmax}}(i, j) = \frac{\mathbf{H}_n(i, j) - \mathbf{H}_{\min}}{\mathbf{H}_{\max} - \mathbf{H}_{\min}} \in [0, 1],$$

for  $n \in [1, \dots, N]$  given  $N$  samples and  $i, j$  indexing rows/columns of CSI matrices.

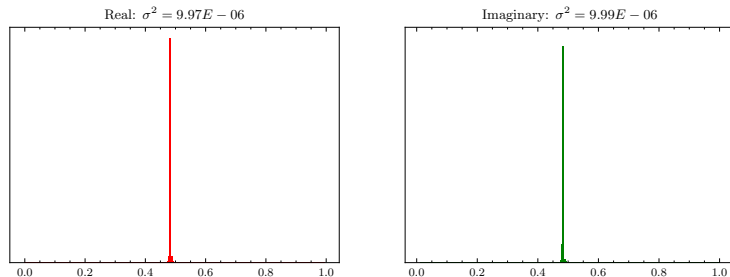


**Figure:** Distribution and variance of minmax-normalized COST2100 real/imaginary channels ( $N = 99000$ ) images.

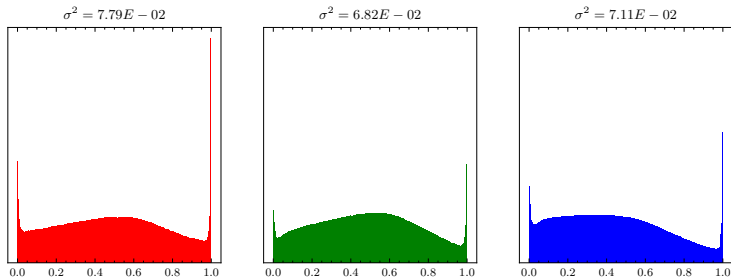


Figure: Distribution and variance of minmax-normalized ImageNet color channels ( $N = 50000$ ) images.



Difference of **four orders of magnitude**.

Dataset	Channels	Normalization	Avg. Variance
ImageNet	RGB	Minmax	<u><math>7.24E^{-2}</math></u>
COST2100	Real, Imag	Minmax	<u><math>9.98E^{-6}</math></u>

**Table:** Minmax normalization applied to COST2100 and ImageNet dataset.

**Spherical normalization** – scale each channel sample by its power,

$$\check{\mathbf{H}}^n = \frac{\mathbf{H}^n}{\|\mathbf{H}^n\|}. \quad (1)$$

After applying (1) to each sample, minmax scaling is applied to the entire dataset.

The resulting dataset under spherical normalization exhibit a larger variance than the same dataset under minmax scaling.

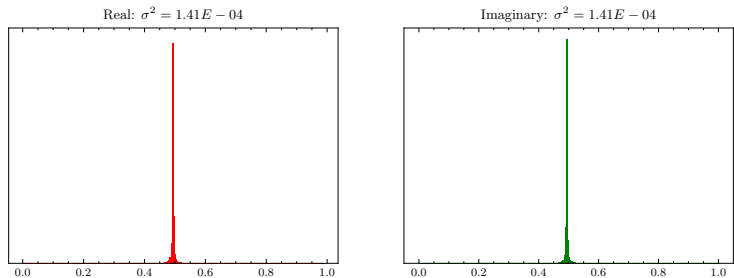


**Figure:** Distribution and variance of COST2100 real/imaginary channels under spherical normalization ( $N = 99000$ ) images.

Under Spherical Normalization, difference is now **two orders of magnitude**.

Dataset	Channels	Normalization	Avg. Variance
ImageNet	RGB	Minmax	$\underline{7.24E^{-2}}$
COST2100	Real, Imag	Spherical	$\underline{1.41E^{-4}}$
COST2100	Real, Imag	Minmax	$9.98E^{-6}$

**Table:** Minmax vs. spherical normalization applied to COST2100 datasets compared with ImageNet.

Under spherical normalization, MSE loss becomes equivalent to NMSE.  
Recall the definitions,

$$\text{MSE} = \frac{1}{N} \sum_{k=1}^N \|\mathbf{H}_k - \hat{\mathbf{H}}_k\|^2, \quad \text{NMSE} = \frac{1}{N} \sum_{k=1}^N \frac{\|\mathbf{H}_k - \hat{\mathbf{H}}_k\|^2}{\|\mathbf{H}_k\|^2}$$

Under spherical normalization, MSE loss becomes equivalent to NMSE.  
Recall the definitions,

$$\text{MSE} = \frac{1}{N} \sum_{k=1}^N \|\mathbf{H}_k - \hat{\mathbf{H}}_k\|^2, \quad \text{NMSE} = \frac{1}{N} \sum_{k=1}^N \frac{\|\mathbf{H}_k - \hat{\mathbf{H}}_k\|^2}{\|\mathbf{H}_k\|^2}$$

The MSE of the spherically normalized estimator is equivalent to the NMSE of the regular estimator, i.e.

$$\begin{aligned} \text{MSE}_{\text{Sph}} &= \frac{1}{N} \sum_{k=1}^N \|\check{\mathbf{H}}_k - \hat{\mathbf{H}}_k\|^2 \\ &= \frac{1}{N} \sum_{k=1}^N \left\| \frac{\mathbf{H}_k}{\|\mathbf{H}_k\|} - \frac{\hat{\mathbf{H}}_k}{\|\mathbf{H}_k\|} \right\|^2 \\ &= \frac{1}{N} \sum_{k=1}^N \frac{\|\mathbf{H}_k - \hat{\mathbf{H}}_k\|^2}{\|\mathbf{H}_k\|^2} \quad \square. \end{aligned}$$

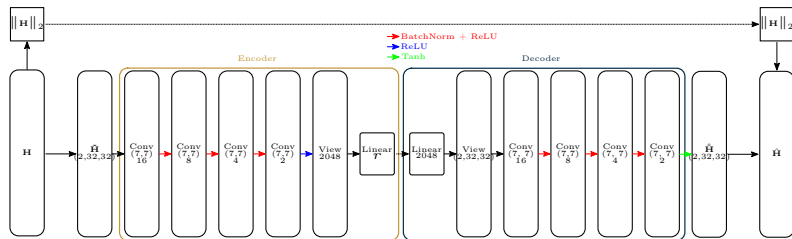


**Figure:** SphNet – CsiNetPro architecture with Spherical Normalization.

---

Z. Liu, **M. del Rosario**, X. Liang, L. Zhang, and Z. Ding, “Spherical normalization for learned compressive feedback in massive mimo csi acquisition,” in *2020 IEEE International Conference on Communications Workshops (ICC Workshops)*, pp. 1–6, 2020

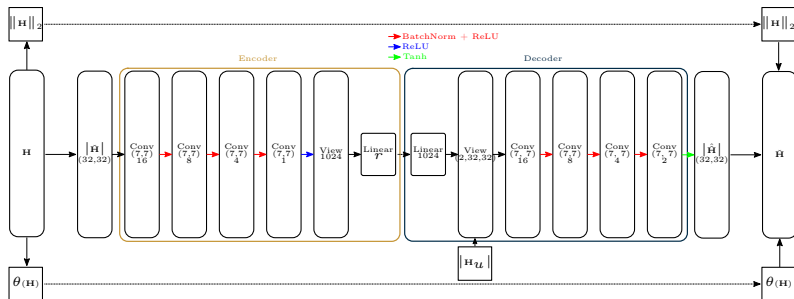


Figure: DualNet-Sph – CsiNetPro architecture with Spherical Normalization and Bidirectional Reciprocity.



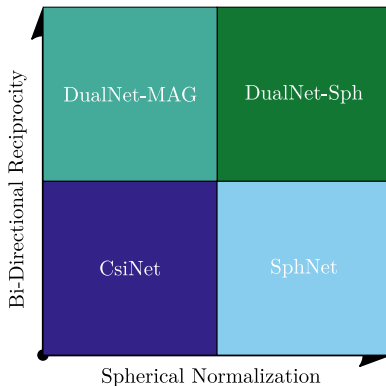


Figure: Illustration of techniques used in different models.

---

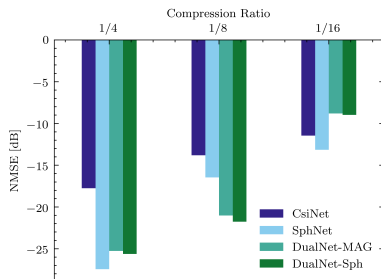
Z. Liu, **M. del Rosario**, X. Liang, L. Zhang, and Z. Ding, “Spherical normalization for learned compressive feedback in massive mimo csi acquisition,” in *2020 IEEE International Conference on Communications Workshops (ICC Workshops)*, pp. 1–6, 2020

Two MIMO scenarios using COST 2100 model with 32 antennas at gNB and single UE (single antenna), 1024 subcarriers.

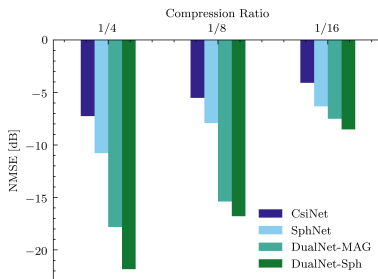
1. **Indoor** environment using 5.3GHz, 0.1 m/s UE mobility, square area of length 20m
2. **Outdoor** environment using 300MHz, 1 m/s UE mobility, square area of length 400m

**Dataset:**  $10^5$  channel samples – 70%/30% training/test split.

**Hyperparameters:** Adam optimizer with learning rate  $10^{-3}$ , batch size 200, 1000 epochs, MSE loss



(a) Indoor



(b) Outdoor

**Figure:** NMSE (lower is better) comparison of bidirectional reciprocity and spherical normalization against CsiNet for increasing compression ratio [4]

---

Z. Liu, M. del Rosario, X. Liang, L. Zhang, and Z. Ding, "Spherical normalization for learned compressive feedback in massive mimo csi acquisition," in *2020 IEEE International Conference on Communications Workshops (ICC Workshops)*, pp. 1–6, 2020

## Prior Work #2: MarkovNet

---

A deep differential autoencoder for efficient temporal learning.

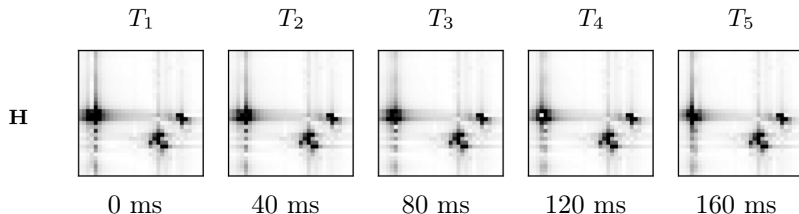


**Figure:** Ground truth CSI (**H**) for five timeslots ( $T_1$  through  $T_5$ ) on one outdoor sample from the validation set.

Recurrent neural networks (RNNs) contain trainable long short-term memory (LSTM) cells which learn temporal relationships.

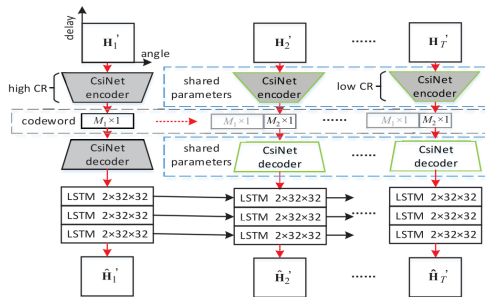


Figure: CsiNet-LSTM network architecture [6].

LSTMs improve NMSE at smaller compression ratios.

		CR	LASSO	BM3D-AMP	TVAL3	CsiNet	CsiNet-LSTM
Indoor	NMSE	1/16	-2.96	0.25	-3.20	-10.59	<b>-23.06</b>
		1/32	-1.18	20.85	-0.46	-7.35	<b>-22.33</b>
		1/64	-0.18	26.66	0.60	-6.09	<b>-21.24</b>
	$\rho$	1/16	0.72	0.29	0.73	0.95	<b>0.99</b>
		1/32	0.53	0.17	0.45	0.90	<b>0.99</b>
		1/64	0.30	0.16	0.24	0.87	<b>0.99</b>
	runtime	1/16	0.2471	0.3454	0.3148	<b>0.0001</b>	0.0003
		1/32	0.2137	0.5556	0.3148	<b>0.0001</b>	0.0003
		1/64	0.2479	0.6047	0.2860	<b>0.0001</b>	0.0003
	NMSE↓	1/16-1/64	94%	105	1.19	42%	<b>8%</b>
Outdoor	NMSE	1/16	-1.09	0.40	-0.53	-3.60	<b>-9.86</b>
		1/32	-0.27	18.99	0.42	-2.14	<b>-9.18</b>
		1/64	-0.06	24.42	0.74	-1.65	<b>-8.83</b>
	$\rho$	1/16	0.49	0.23	0.46	0.75	<b>0.95</b>
		1/32	0.32	0.16	0.28	0.63	<b>0.94</b>
		1/64	0.19	0.16	0.19	0.58	<b>0.93</b>
	runtime	1/16	0.2122	0.4210	0.3145	<b>0.0001</b>	0.0003
		1/32	0.2409	0.6031	0.2985	<b>0.0001</b>	0.0003
		1/64	0.0166	0.5980	0.2850	<b>0.0001</b>	0.0003
	NMSE↓	1/16-1/64	94%	60	2.40	54%	<b>10%</b>

---

T. Wang, C. Wen, S. Jin, and G. Y. Li, “Deep Learning-Based CSI Feedback Approach for Time-Varying Massive MIMO Channels,” *IEEE Wireless Comm. Letters*, vol. 8, pp. 416–419, April 2019

**Problem:** Number of parameters/FLOPs for RNNs is large.

**Table:** Model size and computational complexity of CsiNet-LSTM and CsiNet. M: million.

	Parameters		FLOPs	
CR	CsiNet-LSTM	CsiNet	CsiNet-LSTM	CsiNet
1/4	132.7 M	2.1 M	412.9 M	7.8 M
1/8	123.2 M	1.1 M	410.8 M	5.7 M
1/16	118.5 M	0.5 M	409.8 M	4.7 M
1/32	116.1 M	0.3 M	409.2 M	4.1 M
1/64	115.0 M	0.1 M	409.0 M	3.9 M



Instead of learning a temporal dependency across multiple timeslots, we proposed a **one-step differential encoder**.

For short enough feedback intervals between  $t$  and  $t - 1$ , we view CSI data as a Markov chain, i.e.

$$\mathbf{H}_t = \gamma \mathbf{H}_{t-1} + \mathbf{V}_t,$$

with  $\gamma \in \mathbb{R}^+$  and i.i.d  $\mathbf{V}_t$  such that  $\mathbf{V}_t \sim \mathcal{CN}(\mathbf{0}, \Sigma_V)$ .

---

Z. Liu †, M. del Rosario †, and Z. Ding, “A Markovian Model-Driven Deep Learning Framework for Massive MIMO CSI Feedback,” *arXiv e-prints*, Sept.

2020. Submitted to IEEE Transactions on Wireless Communications († equal contribution)

The ordinary least-squares solution,  $\gamma$ , is given as

$$\gamma = \frac{\text{Trace}(\mathbb{E} [\mathbf{H}_{t-1}^H \mathbf{H}_t])}{\mathbb{E} \|\mathbf{H}_t^H \mathbf{H}_t\|^2}.$$

The ordinary least-squares solution,  $\gamma$ , is given as

$$\gamma = \frac{\text{Trace}(\mathbb{E} [\mathbf{H}_{t-1}^H \mathbf{H}_t])}{\mathbb{E} \|\mathbf{H}_t^H \mathbf{H}_t\|^2}.$$

We utilize the estimator,  $\hat{\gamma}$ , based on the second-order statistics of the CSI matrices,

$$\hat{\gamma} = \frac{\sum_{i=1}^N \text{Trace}([\mathbf{H}_{t-1}^H(i) \mathbf{H}_t(i)])}{\sum_{i=1}^N \|\mathbf{H}_t^H(i) \mathbf{H}_t(i)\|^2},$$

for training set of size  $N$ .

With the one-step estimator  $\hat{\gamma}$ , we propose train an encoder for the estimation error as

$$\mathbf{s}_t = f_{e,t}(\mathbf{H}_t - \hat{\gamma}\hat{\mathbf{H}}_{t-1}),$$

and we jointly train a decoder,

$$\hat{\mathbf{H}}_t = f_{d,t}(\mathbf{s}_t) + \hat{\gamma}\hat{\mathbf{H}}_{t-1}$$

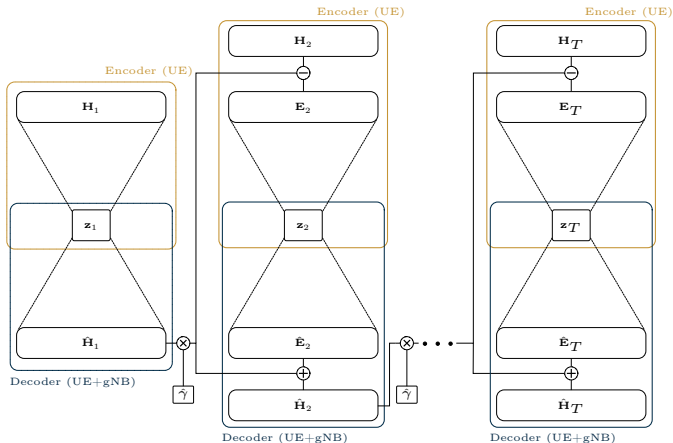
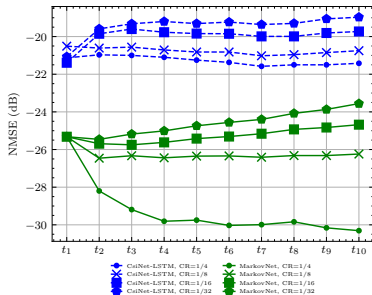
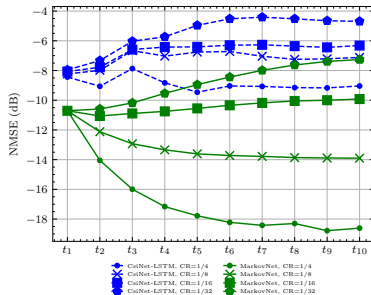


Figure: Abstract architecture for MarkovNet. Networks at  $t \geq 2$  are trained to predict the estimation error,  $E_t$ .



(a) Indoor



(b) Outdoor

Figure: NMSE comparison of MarkovNet and CsiNet-LSTM at various compression ratios (CR).

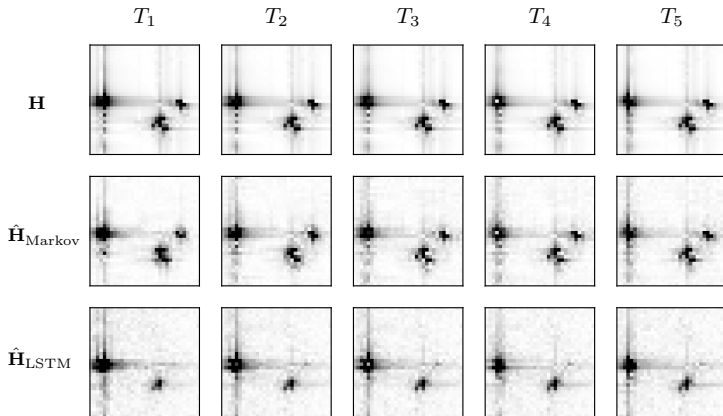


**Figure:** Ground truth CSI ( $\mathbf{H}$ ), MarkovNet estimates ( $\hat{\mathbf{H}}_{\text{Markov}}$ ), and CsiNet-LSTM estimates ( $\hat{\mathbf{H}}_{\text{LSTM}}$ ) for five timeslots ( $T_1$  through  $T_5$ ) on one outdoor sample from the test set (both networks at  $\text{CR} = \frac{1}{4}$ ).

**Table:** Model size/computational complexity of tested temporal networks (CsiNet-LSTM, MarkovNet) and comparable non-temporal network (CsiNet). M: million.

	Parameters		
	CsiNet-LSTM	MarkovNet	CsiNet
<b>CR=1/4</b>	132.7 M	2.1 M	2.1 M
<b>CR=1/8</b>	123.2 M	1.1 M	1.1 M
<b>CR=1/16</b>	118.5 M	0.5 M	0.5 M
<b>CR=1/32</b>	116.1 M	0.3 M	0.3 M
<b>CR=1/64</b>	115.0 M	0.1 M	0.1 M
	FLOPs		
	CsiNet-LSTM	MarkovNet	CsiNet
<b>CR=1/4</b>	412.9 M	44.5 M	7.8 M
<b>CR=1/8</b>	410.8 M	42.4 M	5.7 M
<b>CR=1/16</b>	409.8 M	41.3 M	4.7 M
<b>CR=1/32</b>	409.2 M	40.8 M	4.1 M
<b>CR=1/64</b>	409.0 M	40.5 M	3.9 M



# Proposed Work: CsiNet-SoftQuant

---

An end-to-end trained autoencoder with learned feedback quantization.

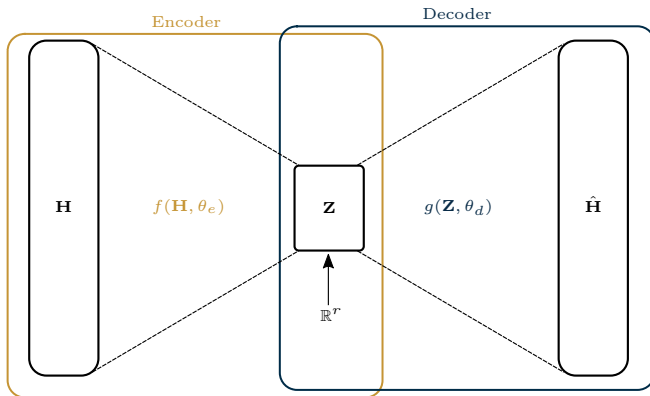


**Figure:** Autoencoder architecture with  $r$ -dimensional real-valued latent feedback elements.

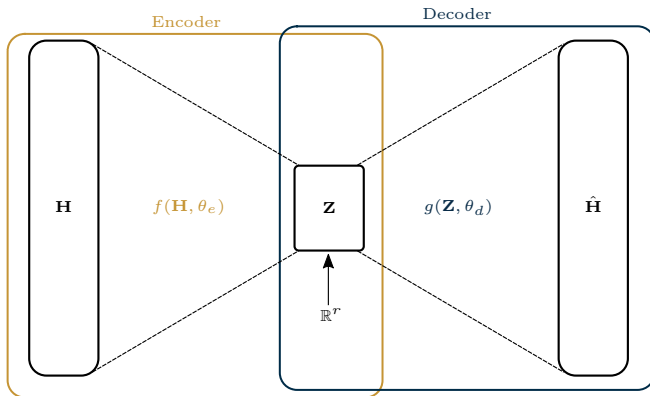


**Figure:** Autoencoder architecture with  $r$ -dimensional real-valued latent feedback elements.

**Problem:** Feedback elements must be discrete-valued. How to quantize?

Network with uniform quantization and arithmetic encoding of latent vectors.

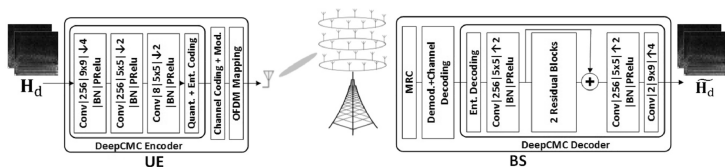


**Figure:** Architecture for DeepCMC [8]. Network uses entropy encoding of uniform quantized feedback elements to minimize bit rate.

---

Q. Yang, M. B. Mashhadi, and D. Gündüz, “Deep convolutional compression for massive mimo csi feedback,” in *2019 IEEE 29th International Workshop on Machine Learning for Signal Processing (MLSP)*, pp. 1–6, 2019

Network with uniform quantization and arithmetic encoding of latent vectors.

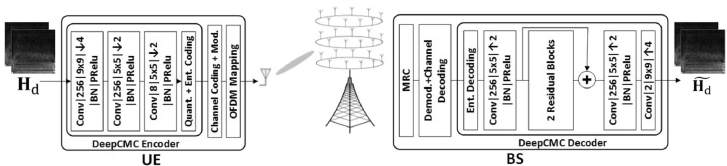


**Figure:** Architecture for DeepCMC [8]. Network uses entropy encoding of uniform quantized feedback elements to minimize bit rate.

*Is fixed quantization scheme optimal?*

---

Q. Yang, M. B. Mashhadi, and D. Gündüz, "Deep convolutional compression for massive mimo csi feedback," in *2019 IEEE 29th International Workshop on Machine Learning for Signal Processing (MLSP)*, pp. 1–6, 2019

We propose to use soft-to-hard vector quantization (SHVQ) [9]. Define the  $m$ -dimensional codebook of size  $L$  as  $\mathbf{C} \in \mathbb{R}^{m \times L}$ . The soft vector assignments of the  $j$ -th latent vector  $\tilde{\mathbf{z}}_j$  can be written as,

$$\phi(\tilde{\mathbf{z}}_j) = \left[ \frac{\exp(-\sigma \|\tilde{\mathbf{z}}_j - \mathbf{c}_\ell\|^2)}{\sum_{i=1}^L \exp(-\sigma \|\tilde{\mathbf{z}}_j - \mathbf{c}_i\|^2)} \right]_{\ell \in [L]} \in \mathbb{R}^L, \quad (2)$$

which is referred to as the ‘softmax’ function.  $\sigma$  is a *temperature* or *annealing* parameter which controls the degree of quantization,

$$\lim_{\sigma \rightarrow \infty} \phi(\tilde{\mathbf{z}}_j) = \text{onehot}(\tilde{\mathbf{z}}_j) = \begin{cases} 1 & \ell = \underset{\ell}{\operatorname{argmax}} \phi(\tilde{\mathbf{z}}_j)[\ell] \\ 0 & \text{otherwise} \end{cases} \quad (3)$$

---

E. Agustsson, F. Mentzer, M. Tschannen, L. Cavigelli, R. Timofte, L. Benini, and L. Van Gool, “Soft-to-hard vector quantization for end-to-end learning compressible representations,” *Advances in Neural Information Processing Systems*, vol. 2017-Decem, no. Nips, pp. 1142–1152, 2017

The soft assignments  $\phi$  admit probability masses over the codewords,

$$q_j = \phi(\tilde{\mathbf{z}}_j).$$

Based on finite samples, we define the histogram probability estimates  $p_j$

$$p_j = \frac{|\{e_l(\mathbf{z}_i) | l \in [m], i \in [N], e_l(\mathbf{z}_i) = j\}|}{mN}.$$

Our target for the rate loss is the crossentropy between  $p_j$  and  $q_j$  term,

$$H(\phi) := H(p, q) = - \sum_{j=1}^L p_j \log q_j = H(p) + D_{\text{KL}}(p \| q).$$

Loss function for soft quantization = regularized rate-distortion function.

$$\operatorname{argmin}_{\theta_e, \theta_d, \mathbf{C}} L_d(\mathbf{H}, \hat{\mathbf{H}}) + \lambda L_{\ell^2}(\theta_e, \theta_d, \mathbf{C}) + \beta L_r(\theta_e, \mathbf{C}) \quad (4)$$

Where the different loss terms are

Term	Definition	Description
$L_d(\mathbf{H}, \hat{\mathbf{H}})$	$\frac{1}{N} \sum_{i=1}^N \ \mathbf{H}_i - g(Q(f(\mathbf{H}_i, \theta_e), \mathbf{C}), \theta_d)\ ^2$	distortion loss
$L_{\ell^2}(\theta_e, \theta_d, \mathbf{C})$	$\ \theta_e\ ^2 + \ \theta_d\ ^2 + \ \mathbf{C}\ ^2$	$\ell^2$ penalty
$L_r(\theta_e, \mathbf{C})$	$mH(\phi)$	rate loss



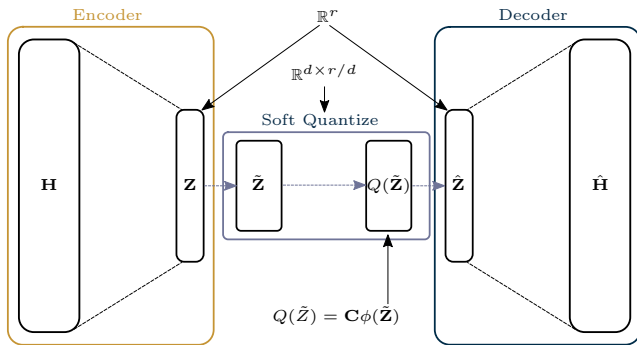


**Figure:** Abstract architecture for CsiNet-SoftQuant [8]. SoftQuantize layer ( $Q(\tilde{\mathbf{Z}})$ ) is a continuous, softmax-based relaxation of a  $d$ -dimensional quantization of the latent layer  $\mathbf{Z}$ .

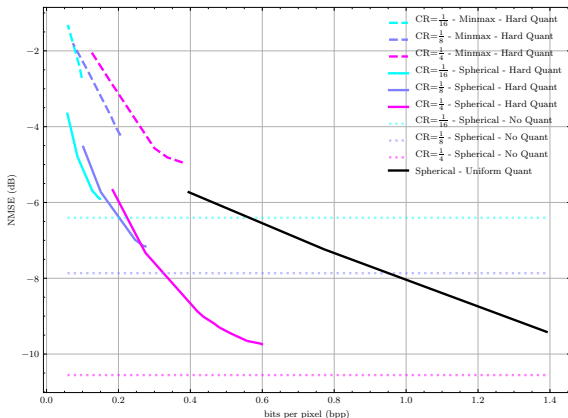


**Figure:** Rate distortion of CsiNet-SoftQuant under both minmax (dotted line) and spherical (solid line) normalization using:  $L = 1024$  centers,  $d = 4$ . Hard quantization performance shown for each CR.

Given angular-delay domain CSI data,  $\mathbf{H}$ , assume i.i.d.  $\mathbf{H}_{(i,j)}$  for  $i$ -th ( $j$ -th) row (col).

Given angular-delay domain CSI data,  $\mathbf{H}$ , assume i.i.d.  $\mathbf{H}_{(i,j)}$  for  $i$ -th ( $j$ -th) row (col).

Denote the quantized CSI matrix,  $\mathbf{H}^\Delta$ , quantized with  $b$  bits. The entropy of the  $(i, j)$ -th element is

$$H(\mathbf{H}_{(i,j)}^\Delta) = - \sum_k^{2^b} p(\mathbf{H}_{(i,j)}^\Delta = k) \log p(\mathbf{H}_{(i,j)}^\Delta = k),$$

where  $p(\mathbf{H}_{(i,j)}^\Delta = k)$  can be obtained as a histogram estimate over the entire dataset.

Given angular-delay domain CSI data,  $\mathbf{H}$ , assume i.i.d.  $\mathbf{H}_{(i,j)}$  for  $i$ -th ( $j$ -th) row (col).

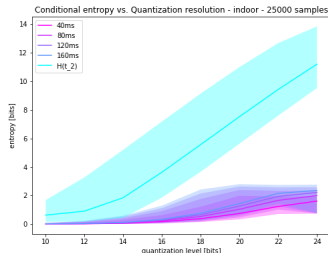
Denote the quantized CSI matrix,  $\mathbf{H}^\Delta$ , quantized with  $b$  bits. The entropy of the  $(i, j)$ -th element is

$$H(\mathbf{H}_{(i,j)}^\Delta) = - \sum_k^{2^b} p(\mathbf{H}_{(i,j)}^\Delta = k) \log p(\mathbf{H}_{(i,j)}^\Delta = k),$$

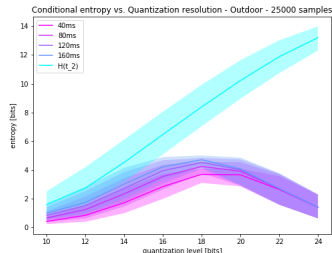
where  $p(\mathbf{H}_{(i,j)}^\Delta = k)$  can be obtained as a histogram estimate over the entire dataset.

A conservative upper bound on the entropy of the full CSI matrix is

$$H(\mathbf{H}^\Delta) = \frac{1}{R_d n_T} \sum_i^{R_d} \sum_j^{n_T} H(\mathbf{H}_{(i,j)}^\Delta).$$



(a) Indoor



(b) Outdoor

Figure: Mean entropy/conditional entropy estimates  $H(\mathbf{H}^\Delta)$  with 95% c.i. for quantized i.i.d COST2100 elements vs. quantization level (bits).

Again, assume i.i.d.  $\mathbf{H}_{(i,j)}$  for  $i$ -th ( $j$ -th) row (col).

Again, assume i.i.d.  $\mathbf{H}_{(i,j)}$  for  $i$ -th ( $j$ -th) row (col).

The differential entropy of the  $(i,j)$ -th element is

$$\hat{h}(\mathbf{H}_{(i,j)}) = - \int p(\mathbf{H}(i,j) = k) \log p(\mathbf{H}_{(i,j)} = k) dk,$$



Again, assume i.i.d.  $\mathbf{H}_{(i,j)}$  for  $i$ -th ( $j$ -th) row (col).

The differential entropy of the  $(i, j)$ -th element is

$$\hat{h}(\mathbf{H}_{(i,j)}) = - \int p(\mathbf{H}(i, j) = k) \log p(\mathbf{H}_{(i,j)} = k) dk,$$

In practice, the distribution  $p(\mathbf{H}(i, j))$  is difficult to obtain. We can instead resort to the Kozachenko–Leonenko (KL) estimator [10] for each element in  $\mathbf{H}$  and average over the elements,

$$\hat{h}(\mathbf{H}) = \frac{1}{R_d n_T} \sum_i^{R_d} \sum_j^{n_T} \hat{h}(\mathbf{H}_{(i,j)}),$$

for KL estimator  $\hat{h}$ .

---

L. Kozachenko and N. N. Leonenko, “Sample estimate of the entropy of a random vector,” *Problemy Peredachi Informatsii*, vol. 23, no. 2, pp. 9–16, 1987

Based on Theorem 8.3.1 from Cover [11], – for sufficiently small quantization interval  $\Delta = \frac{1}{2^n}$ , the entropy of a quantized random variable is related to its differential entropy as,

$$H(\mathbf{H}^\Delta) = h(\mathbf{H}) + n,$$

for  $n$ -bit quantization. Thus, the differential entropy estimator admits an estimate for the entropy of the quantized CSI,  $\hat{\mathbf{H}}^\Delta$ .

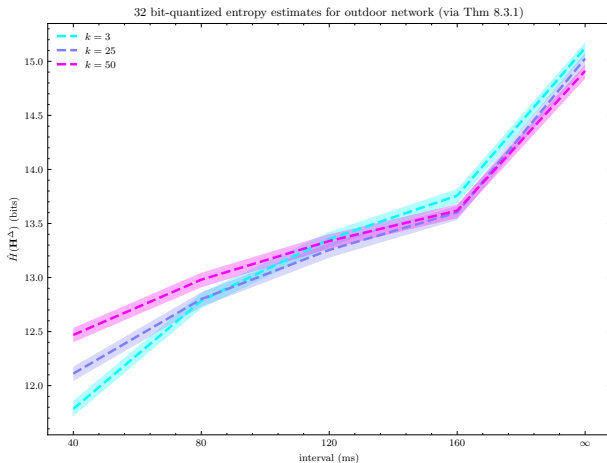


**Figure:** Mean entropy/conditional entropy estimates  $\hat{H}(\mathbf{H}^\Delta) = \hat{h}(\mathbf{H}) + n$  with 95% c.i. for quantized i.i.d COST2100 elements vs. quantization level (bits).

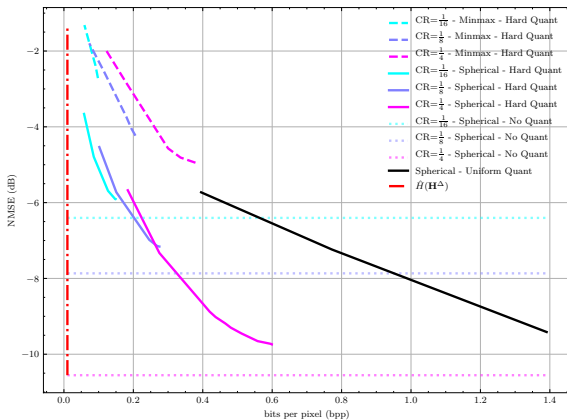


Figure: Rate distortion of CsiNet-SoftQuant with current entropy bound based on  $\hat{H}(\mathbf{H}^\Delta)$ .

Questions?

`mdelrosa@ucdavis.edu`

---

- [1] E. Crespo Marques, N. Maciel, L. Naviner, H. Cai, and J. Yang, "A review of sparse recovery algorithms," *IEEE Access*, vol. 7, pp. 1300–1322, 2019.
- [2] E. C. Marques, N. Maciel, L. A. B. Naviner, H. Cai, and J. Yang, "Compressed sensing for wideband hf channel estimation," in *2018 4th International Conference on Frontiers of Signal Processing (ICFSP)*, pp. 1–5, 2018.
- [3] C. Wen, W. Shih, and S. Jin, "Deep learning for massive mimo csi feedback," *IEEE Wireless Communications Letters*, vol. 7, pp. 748–751, Oct 2018.
- [4] Z. Liu, M. del Rosario, X. Liang, L. Zhang, and Z. Ding, "Spherical normalization for learned compressive feedback in massive mimo csi acquisition," in *2020 IEEE International Conference on Communications Workshops (ICC Workshops)*, pp. 1–6, 2020.
- [5] Z. Liu, L. Zhang, and Z. Ding, "Exploiting Bi-Directional Channel Reciprocity in Deep Learning for Low Rate Massive MIMO CSI Feedback," *IEEE Wireless Communications Letters*, vol. 8, no. 3, pp. 889–892, 2019.
- [6] T. Wang, C. Wen, S. Jin, and G. Y. Li, "Deep Learning-Based CSI Feedback Approach for Time-Varying Massive MIMO Channels," *IEEE Wireless Comm. Letters*, vol. 8, pp. 416–419, April 2019.
- [7] Z. Liu <sup>†</sup>, M. del Rosario <sup>†</sup>, and Z. Ding, "A Markovian Model-Driven Deep Learning Framework for Massive MIMO CSI Feedback," *arXiv e-prints*, Sept. 2020.  
  
Submitted to IEEE Transactions on Wireless Communications.
- [8] Q. Yang, M. B. Mashhadi, and D. Gündüz, "Deep convolutional compression for massive mimo csi feedback," in *2019 IEEE 29th International Workshop on Machine Learning for Signal Processing (MLSP)*, pp. 1–6, 2019.
- [9] E. Agustsson, F. Mentzer, M. Tschannen, L. Cavigelli, R. Timofte, L. Benini, and L. Van Gool, "Soft-to-hard vector quantization for end-to-end learning compressible representations," *Advances in Neural Information Processing Systems*, vol. 2017-Decem, no. Nips, pp. 1142–1152, 2017.
- [10] L. Kozachenko and N. N. Leonenko, "Sample estimate of the entropy of a random vector," *Problemy Peredachi Informatsii*, vol. 23, no. 2, pp. 9–16, 1987.

# Appendix

---

Rather than scalar  $\hat{\gamma} \in \mathbb{R}^+$ , we can derive a multivariate  $p$ -step predictor,  $\mathbf{W}_1, \dots, \mathbf{W}_p$ . Given  $p$  prior CSI samples, the mean-square optimal predictor  $\hat{H}_t$  is a linear combination of these the prior CSI samples,

$$\hat{\mathbf{H}}_t = \mathbf{H}_{t-1} \mathbf{W}_1 + \dots + \mathbf{H}_{t-p} \mathbf{W}_p + \mathbf{E}_t. \quad (5)$$



Error terms are uncorrelated with the CSI samples (i.e.  $\mathbf{H}_{t-i}^H \mathbf{E}_t = 0$  for all  $i \in [0, \dots, p]$ ), and we pre-multiply by  $\mathbf{H}_{t-i}^H$ ,

$$\begin{aligned}\mathbf{H}_{t-i}^H \hat{\mathbf{H}}_t &= \mathbf{H}_{t-i}^H \mathbf{H}_{t-1} \mathbf{W}_1 + \dots + \mathbf{H}_{t-i}^H \mathbf{H}_{t-p} \mathbf{W}_p + \mathbf{H}_{t-i}^H \mathbf{E}_t \\ &= \mathbf{H}_{t-i}^H \mathbf{H}_{t-1} \mathbf{W}_1 + \dots + \mathbf{H}_{t-i}^H \mathbf{H}_{t-p} \mathbf{W}_p.\end{aligned}\tag{6}$$

Denote the correlation matrix  $\mathbf{R}_i = \mathbb{E}[\mathbf{H}_{t-i}^H \mathbf{H}_t]$ . We presume the CSI matrices are generated by a stationary process, and consequently, they have the following properties:

1.  $\mathbf{R}_i = \mathbb{E}[\mathbf{H}_{t-i}^H \mathbf{H}_t] = \mathbb{E}[\mathbf{H}_t^H \mathbf{H}_{t+i}]$
2.  $\mathbf{R}_i = \mathbf{R}_{-i}^H$

Taking the expectation, we can write (6) as a linear combination of correlation matrices,

$$\mathbf{R}_{i+1} = \mathbf{R}_i \mathbf{W}_1 + \cdots + \mathbf{R}_{i-p+1} \mathbf{W}_p.$$

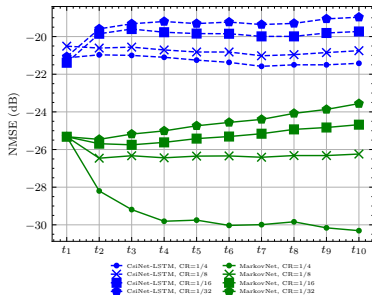
For  $p$  CSI samples, we can write a system of  $p$  equations, which admits the following,

$$\begin{bmatrix} \mathbf{R}_1 \\ \mathbf{R}_2 \\ \vdots \\ \mathbf{R}_p \end{bmatrix} = \begin{bmatrix} \mathbf{R}_0 & \mathbf{R}_1^H & \cdots & \mathbf{R}_{p-1}^H \\ \mathbf{R}_1 & \mathbf{R}_0 & \cdots & \mathbf{R}_{p-2}^H \\ \vdots & & \ddots & \vdots \\ \mathbf{R}_{p-1} & \mathbf{R}_{p-2} & \cdots & \mathbf{R}_0 \end{bmatrix} \begin{bmatrix} \mathbf{W}_1 \\ \mathbf{W}_2 \\ \vdots \\ \mathbf{W}_p \end{bmatrix}.$$

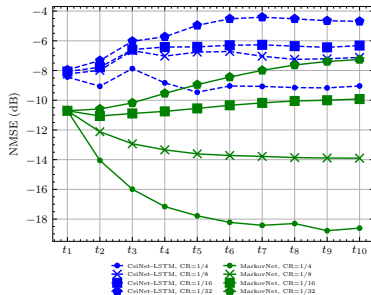
Solving for the coefficient matrices admits the solution

$$\begin{bmatrix} \mathbf{W}_1 \\ \mathbf{W}_2 \\ \dots \\ \mathbf{W}_p \end{bmatrix} = \begin{bmatrix} \mathbf{R}_0 & \mathbf{R}_1^H & \dots & \mathbf{R}_{p-1}^H \\ \mathbf{R}_1 & \mathbf{R}_0 & \dots & \mathbf{R}_{p-2}^H \\ \vdots & & \ddots & \vdots \\ \mathbf{R}_{p-1} & \mathbf{R}_{p-2} & \dots & \mathbf{R}_0 \end{bmatrix}^+ \begin{bmatrix} \mathbf{R}_1 \\ \mathbf{R}_2 \\ \dots \\ \mathbf{R}_p \end{bmatrix}, \quad (7)$$

where  $[\cdot]^+$  denotes the Moore-Penrose pseudoinverse.

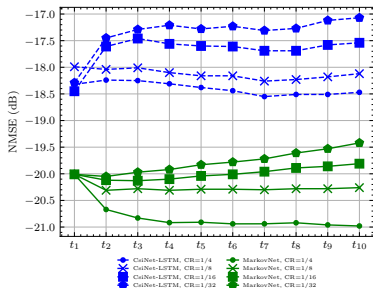


(a) Indoor

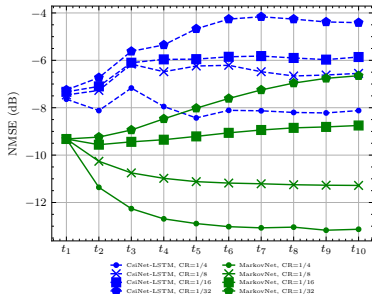


(b) Outdoor

Figure:  $\text{NMSE}_{\text{truncated}}$  comparison of MarkovNet and CsiNet-LSTM at various compression ratios (CR).



(a) Indoor



(b) Outdoor

Figure: NMSE<sub>all</sub> comparison of MarkovNet and CsiNet-LSTM at various compression ratios (CR).

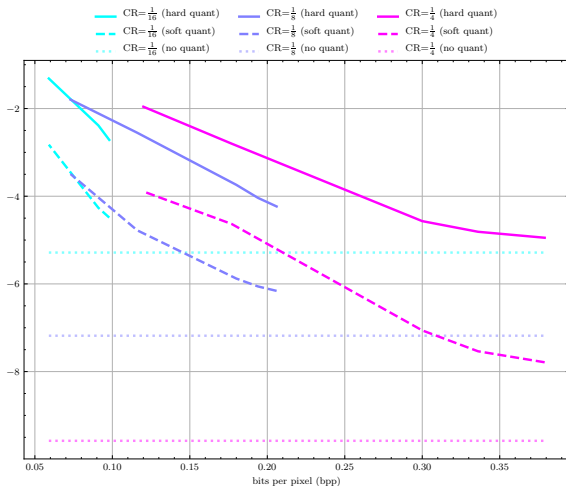


Figure: Rate distortion of CsiNet-SoftQuant under minmax normalization using:  $L = 1024$  centers,  $d = 4$ .

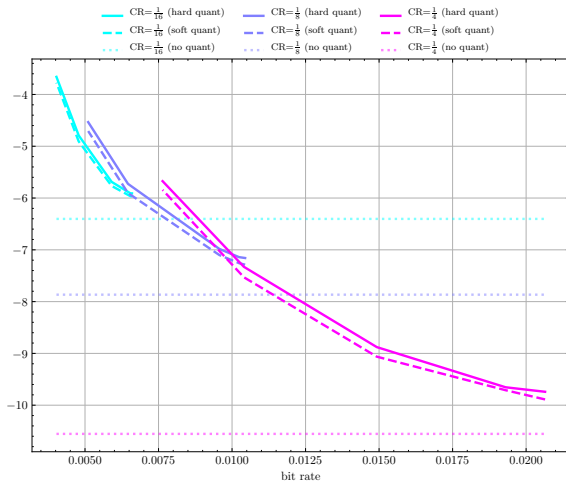
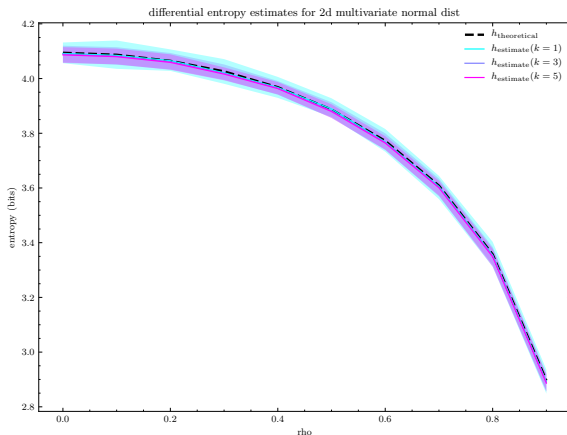


Figure: Rate distortion of CsiNet-SoftQuant using:  $L = 1024$  centers,  $CR = \frac{1}{4}$ ,  $d = 4$ . Bit rates are realized under arithmetic coding of quantized features.





**Figure:** Differential entropy and estimates for 2d multivariate normal distribution. Estimates are based on the KL estimator [10] using the NPEET library [12].